

Spectroscopic strength reduction of intermediate-energy single-proton removal from oxygen isotopes

Y. Z. Sun¹, S. T. Wang^{1,2,*}, Y. P. Xu³, D. Y. Pang⁴, J. G. Li^{1,2}, C. X. Yuan⁵, L. F. Wan⁶, Y. Qiao⁶,
Y. Q. Wang⁶ and X. Y. Chen⁶

¹CAS Key Laboratory of High Precision Nuclear Spectroscopy, Institute of Modern Physics, Chinese Academy of Sciences, Lanzhou 730000, China

²School of Nuclear Science and Technology, University of Chinese Academy of Sciences, Beijing 100049, China

³School of Nuclear Science and Engineering, North China Electric Power University, Beijing 100191, China

⁴School of Physics and Beijing Key Laboratory of Advanced Nuclear Materials and Physics, Beihang University, Beijing 100191, China

⁵Sino-French Institute of Nuclear Engineering and Technology, Sun Yat-Sen University, Zhuhai 519082, China

⁶School of Nuclear Science and Technology, Lanzhou University, Lanzhou 730000, China



(Received 12 June 2022; accepted 13 September 2022; published 28 September 2022)

Measurements of inclusive single-proton removal cross sections from a variety of oxygen isotopes incident at intermediate energies are collected to be compared with Glauber reaction model predictions using shell-model spectroscopic factors between the initial projectile ground state and configurations of the bound core state+valence proton orbit. The collection of data includes a long oxygen isotopic chain spanning over $^{13-20}\text{O}$ and ^{22}O with relatively high beam energies of 305–635 MeV/nucleon, which facilitates a probe into the reaction-model origin of the dependence of the spectroscopic strength reduction factor R_s (the ratio of the experimental over theoretical single-nucleon removal cross sections) on the binding depth ΔS of the removed nucleon, as high beam energies enhance the applicability of the eikonal and sudden approximation that underlie the Glauber model. Our analysis gives R_s values that largely conform to the former R_s - ΔS systematics established upon data mainly over beam energies of 80–240 MeV/nucleon, yet with a slightly dampened R_s - ΔS dependence, and also signs of an odd-even staggering of R_s with respect to the projectile mass number A .

DOI: [10.1103/PhysRevC.106.034614](https://doi.org/10.1103/PhysRevC.106.034614)

I. INTRODUCTION

Since the 1950s, the independent particle model (IPM) [1] has been providing indispensable guidance to advancing our understanding of atomic nuclei [2]. IPM assumes in the nucleus an effective mean field generated by the interparticle interactions of the constituent nucleons which move independently of each other. The model has been successful in accounting for shell closures and predicting the spins and parities of nuclei near doubly closed shells. Yet without explicit inclusion of the residual interactions which is the remnant of the mean field approximation, the model overestimates shell occupancies of protons considerably: proton-knockout reactions induced by high-energy electrons [($e, e'p$) experiments] for a wide range of magic and near-magic nuclei measured occupancies that were only 40%–65% of IPM expectations [3]. Modern shell models (SM) taking into account residual interactions involve the diagonalization of a large Hamiltonian matrix representing effective interactions in a truncated model space, which introduces mixing of valence configurations and leads to fragmented shell occupancies spreading over orbits above the Fermi level. The predictive power of SM then is sensitive to the amount of realistic internucleon correlations included in the calculation [3,4], e.g., the long-range cor-

relations (LRC) and the short-range correlations (SRC) [5]. Experimental measurements of the occupancies are expected to provide valuable data for shell models to evolve by improving their choices of residual interactions.

Direct removal (knockout) of one nucleon from stable or radioactive ion beams (RIB) with beam energies ranging from tens to several hundred MeV/nucleon has been developed as a potent tool for nuclear spectroscopy since the 21st century [4], which can access short-lived nuclei and neutron states that are inaccessible with ($e, e'p$) experiments. Accordingly, the number of nucleons in a shell model orbit (shell occupancy) are characterized by the spectroscopic factor C^2S between the initial projectile ground state (g.s.) and the valence configuration of the bound final mass $A - 1$ reaction residue (core) state+the valence nucleon orbit, which is evaluated theoretically as the wave function overlap following Eq. (1) [4]:

$$\begin{aligned} \langle \mathbf{r}, \Psi_{\alpha}^{A-1} | \Psi_{\text{g.s.}}^A \rangle &= \sum_{nlj} c_{nlj,\alpha} \psi_{nlj}(\mathbf{r}), \\ C^2S(\alpha, nlj) &= |c_{nlj,\alpha}|^2, \end{aligned} \quad (1)$$

where α denotes the final bound state of the reaction residue. It is found from Eq. (1) that the spectroscopic factor $C^2S(\alpha, nlj)$ can be treated as the spectroscopic strength of the valence configuration (α, nlj) in the ground state wave function $|\Psi_{\text{g.s.}}^A\rangle$ of the projectile. Then the inclusive single-nucleon removal

*wangshitao@impcas.ac.cn

cross section σ_{th} is expressed as Eq. (2) [6]:

$$\sigma_{\text{th}} = \sum_{\alpha, nlj} \left(\frac{A}{A-1} \right)^N C^2S(\alpha, nlj) \sigma_{\text{sp}}(nlj, S_{\alpha}^*). \quad (2)$$

The $[A/(A-1)]^N$ factor in front of C^2S is a center-of-mass correction [7] with $N = 2n + l = 0, 1, 2, \dots$ the major oscillator quanta of the valence nucleon's single particle orbit. $S_{\alpha}^* = S_{n(p)} + E_{\alpha}^*$ is the effective nucleon separation energy with $S_{n(p)}$ the ground-state-to-ground-state separation energy of the valence neutron (proton), and E_{α}^* the level energy of the core state α with respect to (w.r.t.) its ground state. The sum in Eq. (2) is over all the valence configurations (α, nlj) with bound core state α . σ_{sp} is the so-called single-particle (sp) cross section, calculated using reaction models assuming $\Psi_{\text{g.s.}}^A$ having only one pure (α, nlj) valence configuration, which provides a normalized valence nucleon-core relative wave function ψ_{nlj} [4]. The relatively high beam energy used in knockout reactions enables the treatment of sudden (fast collision) and eikonal (forward scattering) approximations (SE approximation). As one of the prevalent reaction models for knockout reactions on composite (nonproton) target, Glauber model [8] is based on the SE approximation. So high beam energies are crucial to ensure the validity of the reaction theory [9].

With the increasing body of experimental data [10] of single-nucleon knockout induced by fast stable and radioactive beams spanning a wide range of the binding depth of the removed nucleon (represented by ΔS , see Sec. III or Ref. [11] for definition), a universal overestimation of the knockout cross sections, as quantified by the ratio of the experimental over theoretical inclusive one-nucleon knockout cross sections

$$R_s = \frac{\sigma_{\text{exp}}}{\sigma_{\text{th}}} \quad (3)$$

is observed in the whole range of ΔS . Usually referred to as the reduction (quenching) factor of the spectroscopic strengths (factors) in literature despite that whether the overestimation should be ascribed to reaction model or structure theory is not clear yet [12], R_s is further found to have a significant and almost-linear dependence on ΔS [10] that measures the binding of the removed valence nucleon in the projectile, which increases with the neutron (proton) excess for valence proton (neutron) removal. Both experimental and theoretical evidences exist in favor of a neutron-proton asymmetry dependence of internucleon correlations [13,14] experienced by the valence nucleon, whereas they are not satisfactory in accounting for the specific trend and the slope of the almost-linear R_s - ΔS dependence [12]. Besides, experimental probes other than knockout reactions on composite Be and C target reached a disparate R_s - ΔS systematics. (p, d) transfer reactions [15,16] and $(p, 2p)$ quasifree scattering [17–19] both observed no strong dependence of R_s on the proton-neutron asymmetry of the nucleus with shell-model spectroscopic factors as the structural input. This puts more suspicion into the reaction model origin for the R_s - ΔS dependence and in turn the validity of the SE approximation underlying the Glauber model [12]. The data included in Ref. [10] are mainly over

beam energies of 80–240 MeV/nucleon from different labs. High-beam-energy and variable-controlled data will place the SE approximation on an even stronger footing with limited systematic errors, and serve as a valuable addition to the current R_s - ΔS systematics.

Accordingly, this paper carries out a consistent analysis of the inclusive single-proton ($-p$) removal cross sections from a wide range of oxygen isotopes covering $^{13-20}\text{O}$ and ^{22}O with Glauber reaction model calculations using shell-model structural inputs. The theoretical cross sections are compared with experimental data mainly collected from two experiments conducted at the GSI Helmholtzzentrum für Schwerionenforschung (GSI), in Darmstadt, Germany [20,21] at significantly higher beam energies of 305–635 MeV/nucleon. The R_s - ΔS plot is presented and discussed.

II. CALCULATION OF INCLUSIVE ONE-PROTON REMOVAL CROSS SECTIONS

There are certain “standard” and common practices to follow when it comes to the eikonal plus shell model analysis of one-proton knockout reactions, as has been detailed in Ref. [22], and vastly employed, e.g., in Refs. [23–25]. Following Eq. (2), the basic ingredients to calculate the one-nucleon knockout reaction cross section belonging to a specific valence configuration (α, nlj) are the corresponding shell-model spectroscopic factor C^2S following Eq. (1) and the single-particle cross section calculated by the reaction model. We have calculated the C^2S of all the valence configurations (α, nlj) of the removed proton's sp state (nlj) +core bound final state α for $^{13-20}\text{O}$ and ^{22}O using the WBP effective interaction [26] with the code KSHELL [27]. The bound states for each reaction residue are exhausted using their experimental spectra and one-nucleon-emission thresholds from online dataset NuDat [28], and subsequently their counterparts in the corresponding shell-model-calculated states are identified by matching spin parities. We have included all states with nonvanishing spectroscopic factors ($C^2S \geq 0.0001$) as it is worthwhile compared with the entailed additional effort.

The calculation of the single-particle cross section σ_{sp} for the one-proton removal is performed with computer code MOMDIS [29], which implements the Glauber reaction model. σ_{sp} consists of two parts [30], i.e., the stripping or inelastic breakup part σ_{str} , where the removed nucleon is inelastically scattered by the target and leaves the target nucleus excited from its ground state; and the diffractive dissociation or the elastic breakup part σ_{dif} that both the removed nucleon and the core are at most elastically scattered with the target, with usually the stripping as the dominant nucleon removal mechanism [4]. Accordingly, σ_{str} are formulated by Eq. (4) [4],

$$\sigma_{\text{str}} = \frac{1}{2j+1} \int d\mathbf{b} \sum_m \langle \psi_{jm} | (1 - |S_v|^2) | S_c|^2 | \psi_{jm} \rangle, \quad (4)$$

and σ_{dif} by Eq. (5) [4],

$$\sigma_{\text{dif}} = \frac{1}{2j+1} \int d\mathbf{b} \sum_{m,m'} [\langle \psi_{jm} | 1 - |S|^2 | \psi_{jm} \rangle \delta_{m,m'} - |\langle \psi_{jm'} | 1 - |S|^2 | \psi_{jm} \rangle|^2], \quad (5)$$

where S_v and S_c are the valence nucleon-target and core-target elastic S matrices, $S = S_v S_c$, and $\psi_{jm} \equiv \psi_{nljm}$ is the valence nucleon-core relative wave function. The integration is over impact parameter b . The above formulas for σ_{str} and σ_{dif} have very intuitive interpretations. With the notion that $|S_{v(c)}|^2$ is the probability that the valence nucleon (core) survives the reaction (at most elastically scattered with the target nucleus), the integrand of Eq. (4) reads that the probability of one-nucleon knockout via stripping mechanism at impact parameter b is the expectation value of the product of the probabilities that the core survives the reaction (in $|S_c|^2$), and the valence nucleon is absorbed (in $1 - |S_v|^2$) [30]. One can find the explanation for σ_{dif} in, e.g., Refs. [4,30].

The S matrix is calculated from the scattering optical potential between the two scatterers by $S(b) = \exp[i\chi(b)]$, with $\chi(b)$ the eikonal phase

$$\chi(b) = -\frac{1}{2k_{NN}} \frac{2\mu}{\hbar^2} \int dz V(b, z), \quad (6)$$

where μ is the reduced mass, $V(b, z)$ the optical potential and k_{NN} the nucleon-nucleon (NN) momentum. In the optical limit of the Glauber model as has been adopted in present work, $V(b, z)$ is built via the t - ρ - ρ approximation following Eq. (7) [29]:

$$\chi(b) = \frac{1}{k_{NN}} \int dq q \rho_p(q) \rho_t(q) f_{NN}(q) J_0(qb) \quad (7)$$

with $J_0(qb)$ the zeroth-order Bessel function of the first kind, and $\rho_{p(t)}(q)$ the Fourier transform of the projectile (target) nucleonic density, which in this work is taken from Hartree-Fock (HF) calculations based on the SkX parametrization [31] for both the target and the projectile nucleus. $f_{NN}(q)$ is the high-energy NN scattering amplitude. A prevalent parametrization is given by [32]

$$f_{NN}(q) = \frac{k_{NN}}{4\pi} \sigma_{NN} (\mathbf{i} + \alpha_{NN}) \exp(-\beta_{NN} q^2), \quad (8)$$

where σ_{NN} is the total NN cross section, for which the fit of Ref. [33] is adopted. Different parametrizations for α_{NN} and β_{NN} exist [32,34,35], covering different incident energy regions. We have adopted the Horiuchi parameter as in Refs. [6,25], that is applicable for beam energies ranging 30 to 1000 MeV/nucleon and agrees better with experiment data [6].

The valence nucleon-core relative wave function $\psi_{nlj}(\mathbf{r})$ is solved numerically by MOMDIS in a nuclear central potential of Woods-Saxon (WS) form plus a spin-orbit interaction and a Coulomb potential, as detailed in Ref. [29]. As has been pointed out in Ref. [22], σ_{sp} is considerably more sensitive to the rms radius $r_{\text{sp}} = \sqrt{\langle \psi_{nlj} | r^2 | \psi_{nlj} \rangle}$ than the specific shape of the WS potential that is determined by its radius r_0 , diffuseness a_0 and the depth V_0 . We have accordingly made a two-dimensional search in the (r_0, V_0) space of the central WS potential so as to generate a bound state wave function ψ_{nlj} that gives $r_{\text{sp}} = [A/(A-1)]^{1/2} r_{\text{HF}}$ [22] with r_{HF} the rms radius of the sp orbit specified by nlj given by the above mentioned HF calculations, and reproduces the effective separation energy S_α^* , simultaneously, by means of a globally convergent Newton-Raphson root-finding routine for

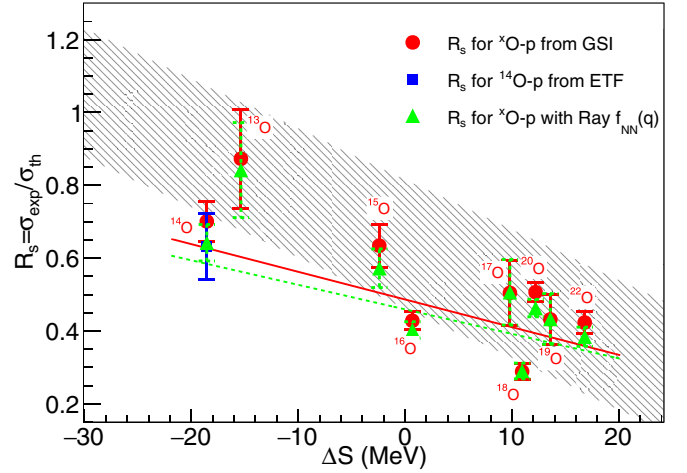


FIG. 1. The R_s - ΔS scatter plot for single-proton removal from $^{13-20}\text{O}$ and ^{22}O at beam energies of 305–635 MeV/nucleon. Experimental cross sections σ_{exp} of the data points are from experiments conducted at GSI [20,21] and ETF [37]. The red and green lines are linear fits to the red and green points, respectively, which share σ_{exp} from GSI and only differs in the choice of $f_{NN}(q)$ parametrization (Horiuchi [35] set for the red points and Ray [32] set for the green points). The hatched area in the background summarizes the totality of the bulk of R_s - ΔS data points from Fig. 1 of Ref. [10].

nonlinear systems of equations [36], which achieves general precision of $|\Delta r_{\text{sp}}| < 0.001$ fm and $|\Delta S_\alpha^*| < 0.001$ MeV for all the valence configurations calculated. As σ_{sp} is relatively more insensitive to other parameters, similar to Ref. [22], we use the same r_0 as with the central potential for the spin-orbit interaction using a fixed depth $V_{S0} = 7.5$ MeV, and the same r_0 for the Coulomb potential. A fixed $a_0 = 0.7$ fm is used for both the central and the spin-orbit interaction.

III. RESULTS AND DISCUSSION

With the theoretical prescription described in Sec. II, the reaction cross sections for one-proton removal from $^{13-20}\text{O}$ and ^{22}O on a carbon target at beam energies over 305–635 MeV/nucleon are calculated and tabulated in Table I, together with the corresponding measurements mainly from experiments conducted at GSI [20,21]. We have also included a data point for $^{14}\text{O}(-p)$ at 305 MeV/nucleon from the External Target Facility (ETF), Institute of Modern Physics, Lanzhou, China [37] for comparison purposes. For each oxygen isotope, the binding depth ΔS of the removed proton is calculated as $\Delta S = S_p + \bar{E}^* - S_n$, where \bar{E}^* is the averaged core excitation energy weighted by the calculated partial cross section to each of all the bound final core states. For orbits that are too highly placed for r_{HF} to be calculated, we have extrapolated the largest r_{HF} available in the oxygen isotope it belongs to. Since these orbits involve configurations with very small spectroscopic strengths, the error brought about by this treatment should be negligibly insignificant.

The R_s calculated according to Eq. (3) are given in the last column of Table I alongside ΔS , and plotted against it in Fig. 1, over a hatched band summarizing the totality of the

TABLE I. Inclusive single-proton removal cross sections of $^{13-20}\text{O}$ and ^{22}O impinging on a carbon target. ($I_c^\pi E_\alpha^*$, nlj) represents bound core state α +valence proton orbit nlj configuration in the projectile ground state. r_{HF} is the rms radius of the valence proton's sp state from HF calculations. σ_{th} are the calculated inclusive single-proton removal cross sections. $\Delta S = S_p + \bar{E}^* - S_n$ indicates the binding depth for the removed proton, with \bar{E}^* the averaged core excitation energy weighted by the calculated partial cross section to each of all the bound final core states. $R_s = \sigma_{\text{exp}}/\sigma_{\text{th}}$ are the reduction factors of the spectroscopic factors with the experimental data σ_{exp} mainly taken from Refs. [20,21]. All the errors are from the experimental data.

Projectile	$E(\text{MeV/nucleon})$	nlj	$r_{\text{HF}}(\text{fm})$	I_c^π	$E_\alpha^*(\text{MeV})$	C^2S	$\sigma_{\text{th}}(\text{mb})$	$\sigma_{\text{exp}}(\text{mb})$	$\Delta S(\text{MeV})$	R_s	
^{13}O	397	$0p_{1/2}$	3.217	1^+	0	0.5291	21.39				
		$0p_{3/2}$	2.829	1^+	0	0.0923	2.87				
		Inclusive				0.6214	24.26	21.56(3.34) [21]	-15.36	0.89(14)	
^{14}O	349	$0p_{1/2}$	3.046	$1/2^-$	0	1.6102	55.16				
		Inclusive				1.6102	55.16	38.65(3.01) [21]	-18.55	0.70(5)	
^{14}O	305	$0p_{1/2}$	3.046	$1/2^-$	0	1.6102	55.30				
		Inclusive				1.6102	55.30	35(5) [37]	-18.55	0.63(9)	
^{15}O	308	$0p_{1/2}$	2.954	1_1^+	0	0.7972	23.58				
				1_2^+	3.948	0.5401	15.91				
				1_3^+	6.204	0.0050	0.15				
				0^+	2.313	0.4052	11.95				
		$0p_{3/2}$	2.776	1_1^+	0	0.2998	7.71				
				1_2^+	3.948	0.3678	9.40				
				1_3^+	6.204	0.0160	0.41				
				2^+	7.029	1.1500	29.30				
				2^-	5.106	0.0358	2.39				
		$0d_{5/2}$	4.111	3^-	5.834	0.0257	1.72				
				$1s_{1/2}$	4.111	0^-	4.915	0.0001	0.01		
				1^-	5.691	0.0074	0.51				
		$0d_{3/2}$	4.111	1^-	5.691	0.0004	0.03				
				Inclusive				3.6505	103.06	65.38(6.06) [21]	-2.41
		^{16}O	450	$0p_{1/2}$	2.903	$1/2^-$	0	1.8049	46.93		
$3/2_1^-$	6.324					3.7203	86.65				
$0p_{3/2}$	2.782			$3/2_2^-$	9.925	0.0251	0.58				
				$0d_{5/2}$	3.370	$5/2_1^+$	5.270	0.0961	3.77		
$0d_{3/2}$	3.370			$5/2_2^+$	7.155	0.0141	0.55				
				$3/2_1^+$	7.301	0.0036	0.14				
$1s_{1/2}$	3.370			$3/2_2^+$	8.571	0.0235	0.92				
				$1/2_1^+$	5.299	0.0081	0.34				
				$1/2_2^+$	8.313	0.0095	0.40				
$1/2_3^+$	9.050			0.0001	0.00						
		Inclusive				5.7053	140.30	60.11(3.38) [21]	0.68	0.43(2)	
^{17}O	629	$0p_{1/2}$	2.872	2^-	0	0.7225	16.99				
				3^-	0.298	1.0365	24.36				
		$0p_{3/2}$	2.780	2^-	0	0.0246	0.53				
				1^-	0.397	0.0070	0.15				
				3^-	0.298	0.0173	0.37				
Inclusive				1.8079	42.41	21.4(3.8) [20]	9.81	0.50(9)			
^{18}O	573	$0p_{1/2}$	2.851	$1/2^-$	0	1.6950	35.47				
				$1/2^-$	3.663	0.0339	0.71				
		$0p_{3/2}$	2.782	$3/2_1^-$	0.374	0.2934	5.79				
				$3/2_2^-$	3.204	0.3697	7.26				
				$3/2_3^-$	5.515	2.5455	49.88				
		$0d_{5/2}$	3.262	$5/2_1^+$	2.526	0.0498	1.54				
				$5/2_2^+$	4.209	0.0450	1.39				
		$1s_{1/2}$	3.262	$1/2^+$	0.850	0.0056	0.19				
$0d_{3/2}$	3.262	$3/2^+$	5.195	0.0034	0.11						
Inclusive					5.0413	102.34	29.6(2.2) [20]	10.96	0.29(2)		
^{19}O	635	$0p_{1/2}$	2.837	2_1^-	0.115	0.6849	13.14				
				2_2^-	0.587	0.0004	0.01				
				3^-	0.742	0.9809	18.80				
		$0p_{3/2}$	2.785	1^-	0	0.0206	0.38				

TABLE I. (Continued.)

Projectile	E (MeV/nucleon)	nlj	r_{HF} (fm)	I_c^π	E_α^* (MeV)	C^2S	σ_{th} (mb)	σ_{exp} (mb)	ΔS (MeV)	R_s
^{20}O	415			2^-	0.587	0.0387	0.71			
				3^-	0.742	0.0020	0.04			
		$0d_{5/2}$	3.239	1^+	2.614	0.0001	0.00			
		$0d_{3/2}$	3.666	1^+	2.614	0.0011	0.04			
		Inclusive				1.7287	33.12	14.3(2.3) [20]	13.60	0.43(7)
		$0p_{1/2}$	2.828	$1/2^-$	0	1.6661	29.40			
		$0p_{3/2}$	2.791	$3/2^-$	1.143	0.4974	8.46			
				$3/2^-$	2.132	0.2763	4.70			
^{22}O	414	$1s_{1/2}$	3.423	$1/2^+$	2.511	0.0073	0.25			
		Inclusive				2.4471	42.80	21.68(1.12) [21]	12.22	0.51(3)
		$0p_{1/2}$	2.818	$1/2^-$	0	1.6315	24.62			
		$0p_{3/2}$	2.805	$3/2^-$	1.160	0.8734	12.99			
		$0d_{5/2}$	3.213	$5/2^+$	2.380	0.0213	0.47			
		Inclusive				2.5262	38.08	16.12(1.10) [21]	16.81	0.42(3)

R_s - ΔS data points included in Fig. 1 of Ref. [10] with beam energies mainly under 240 MeV/nucleon. The figure indicates that the data of single-proton removal from considerably higher-energy oxygen isotopes are still largely amenable to the afore-established R_s - ΔS systematics. As the beam-energy-relevant aspects in the theoretical analysis involve only the validity of the SE approximation and the $f_{NN}(q)$ parametrization in the reaction model, given that the latter reproduces the experimental $^{12}\text{C} + ^{12}\text{C}$ total reaction cross sections well at various energies [6], and together with the work of beam energies mainly below and near 240 MeV/nucleon [10,25], we are tempted to infer that the applicability of the SE approximation in Glauber model, which is expected to vary along beam energy, barely changes up to more than 600 MeV/nucleon.

It also appears that the points in Fig. 1 deviate systematically downwards a little from the center of the hatched area, which may be due to the differences in the theoretical inputs, e.g., the shell-model effective interactions for the calculation of C^2S , the choice for the parametrizations of the NN scattering amplitude $f_{NN}(q)$, and the density of the core and/or the target. This is particularly manifested by the R_s of $^{14}\text{O} - p$ at 305 MeV/nucleon reported as 0.76(11) in Ref. [11] calculated with C^2S taken from Table I of Ref. [9], using the Lenzi [34]-Ray [32] parametrization [22,29] for $f_{NN}(q)$, and a Gaussian for the target density, besides other possible differences in theoretical ingredients that may not have been mentioned here, compared with our value of 0.63(9), which underlines the necessity to perform the analysis for systematic trend with consistent theoretical inputs. The negative linear dependence persists, yet with a slightly dampened slope, as described by a linear fit to the red points (weighted with their respective errors) in Fig. 1, marked by the red straight line of

$$R_s = -0.0076(14)\Delta S + 0.49(2), \quad (9)$$

in comparison with $R_s = -0.016\Delta S + 0.61$ in Ref. [10]. We tried to test this linear representation against the choices of $f_{NN}(q)$ parametrizations by recalculating the red points in Fig. 1 all over again but with Ray parameter set [32]. This only decreases the absolute value of the slope even further, as is

shown by the dashed green line. It is not clear yet whether this suppressed slope is related to the relatively high beam energy range, or the projectiles belonging to the same isotopic chain, or perhaps it is just limited to the oxygen isotopes. More data over lower beam energies (e.g., ≤ 250 MeV/nucleon) with diverse plausible theoretical inputs for oxygen isotopes and similar investigations on other isotopes surely would help to clarify this.

Another feature of Fig. 1 to behold is the staggering of R_s w.r.t. the projectile mass number A alternating odd and even, which has been enhanced by subtracting the linear systematics [Eq. (9)] from R_s and plotting it against A in Fig. 2. With the exception of ^{20}O , R_s are much lower at $^{14,16,18}\text{O}$ than its two neighbors at both sides. As R_s is relatively indifferent to beam energies and this staggering emerges with the increase of neutron number in an oxygen nucleus, we deem its cause as more structure-related than reaction-related. Since the fraction of SRC neutron-proton pairs increases with the neutron excess in the nucleus [13], and the knockout of a proton in an SRC

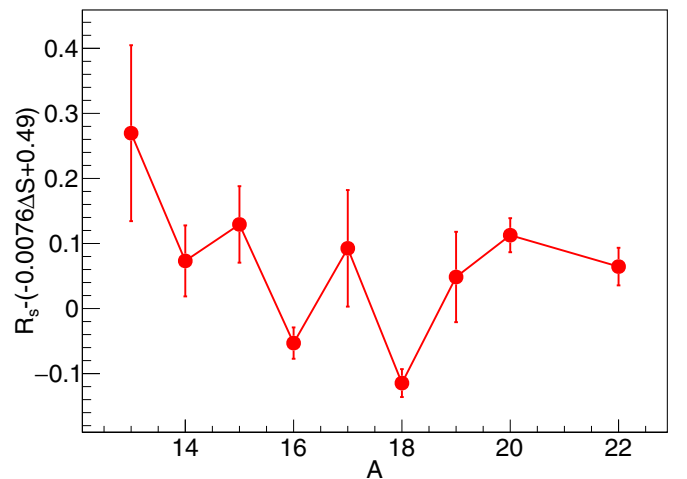


FIG. 2. The odd-even staggering of R_s w.r.t. the projectile mass number A illustrated by $R_s - (0.0076\Delta S + 0.49)$ vs A plot. The lines joining the points are to guide the eye.

pair would leave the correlated neutron to recoil and be ejected as well [5], this odd-even staggering of R_s w.r.t A may signify the missing of certain NN correlations due to nucleon pairing force that has not been properly accounted for in the structural inputs, i.e., the C^2S , or in the valence proton-core relative wave function ψ_{nlj} [38,39] solved in the WS mean-field by MOMDIS, for the even- A oxygen projectiles in the calculation of σ_{th} , which leads to their overestimation.

With accumulating data of heavy-ion induced one-nucleon knockout experiments conducted at high beam energies (in excess of 200 MeV/nucleon) in corroboration of the current R_s - ΔS dependence [10,25,40], the Glauber model exhibits robustness against the beam energy, which suggests that the failing of SE approximation w.r.t. beam energy does not dominate the reason for the R_s - ΔS dependence. In view of this, a comparison of results from one-nucleon knockout on composite targets here with that from (p, pN) quasifree scattering ($N = p$ or n , at 300–450 MeV/nucleon) [17–19] and (p, d) transfer (from Ar isotopes at 33 MeV) [15,16] immediately becomes enlightening, the latter of which both observed weak or no R_s - ΔS dependence, analyzed with shell-model spectroscopic inputs and various reaction models, including eikonal distorted wave impulse approximation (eikonal DWIA) [17,18] and transfer-to-the-continuum (TC) method [19] for (p, pN) quasifree scattering, and adiabatic distorted wave approximation (ADWA) for (p, d) transfer reactions [15]. The difference in the obtained R_s - ΔS systematics highlights the characteristics of the two brand of researching tools, i.e., that they both use shell-model structural inputs, their beam energies are all within appropriate regions (or high enough [17,41]) for the respective reactions to happen, yet with different reaction targets comes with disparate results, that *structureless* proton targets yield R_s that are insensitive to ΔS , while composite targets give significant nearly linear dependence. Note that in Glauber model, multiple scattering and final-state interactions of the core with the target or the knocked-out nucleon are neglected. Since composite targets are more absorptive to the core compared with proton targets, it may more easily excite the core to unbound states. Especially given the fact that the knockout of deeply bound valence nucleon leaves a weakly bound core with spatially extensive wave function, that may not be well represented by the corresponding density from HF calculations, the cross sections of deeply bound valence nucleon knockout are more susceptible to theoretical overestimation compared with knockout of weakly bound valence nucleon. A semiclassical intranuclear cascade (INC) model has been successful in reproducing the

low cross sections of deeply bound valence nucleon removal induced by heavy targets [42], where the reinteractions of the core with the struck nucleon and the target that lead to direct removal of more than one nucleon, and the evaporation of nucleon(s) followed by the core excitation in the scattering processing after the one-nucleon knockout, are explicitly considered. Inclusion of these noneikonal processes in Glauber model seems a very promising start to mitigate the R_s - ΔS dependence.

IV. CONCLUSIONS

The inclusive cross sections of single-proton knockout from $^{13-20}\text{O}$ and ^{22}O over beam energies of 305–635 MeV/nucleon are calculated using the Glauber reaction model with shell-model spectroscopic factors C^2S , and compared with their corresponding experimental data mainly from two experiments conducted at GSI and one data point from ETF, for the reduction factors R_s of C^2S . It is found that the resulting R_s w.r.t. the binding depth ΔS of the removed proton still conform to the earlier published R_s - ΔS systematics, that is established upon data with considerably lower beam energies than our work, which further confirms the minor role of the beam-energy dependence of the applicability of the SE approximation in the Glauber model behind the puzzling R_s - ΔS dependence. Our analysis also presents a slightly dampened slope in the linear representation of R_s against ΔS compared with Ref. [10], and signs of an odd-even staggering of R_s w.r.t. the projectile mass number A , which may carry implications for the Glauber model and the missing correlations in the effective interactions of the shell-model and/or the valence nucleon-core relative wave function. Importance of inclusion of indirect processes in Glauber model is emphasized.

ACKNOWLEDGMENTS

This work was supported by the National Natural Science Foundation of China (Grants No. U1732134, 11575257, and 11305222), the Key Laboratory of High Precision Nuclear Spectroscopy, Institute of Modern Physics, Chinese Academy of Sciences, the Open Research Project of CAS Large Research Infrastructures, and Guangdong Major Project of Basic and Applied Basic Research under Grant No. 2021B0301030006.

-
- [1] M. G. Mayer, *Phys. Rev.* **75**, 1969 (1949).
 - [2] E. Caurier, G. Martínez-Pinedo, F. Nowacki, A. Poves, and A. P. Zuker, *Rev. Mod. Phys.* **77**, 427 (2005).
 - [3] G. J. Kramer, H. P. Blok, and L. Lapikas, *Nucl. Phys. A* **679**, 267 (2001).
 - [4] P. G. Hansen and J. A. Tostevin, *Annu. Rev. Nucl. Part. Sci.* **53**, 219 (2003).
 - [5] R. Subedi *et al.*, *Science* **320**, 1476 (2008).
 - [6] C. Wen *et al.*, *Chin. Phys. C* **41**, 054104 (2017).
 - [7] A.E.L. Dieperink and T. de Forest, *Phys. Rev. C* **10**, 543 (1974).
 - [8] C. A. Bertulani and P. Danielewicz, *Introduction to Nuclear Reactions* (Institute of Physics Publishing, Bristol, Philadelphia, 2004), p. 428
 - [9] F. Flavigny, A. Obertelli, A. Bonaccorso, G. F. Grinyer, C. Louchart, L. Nalpas, and A. Signoracci, *Phys. Rev. Lett.* **108**, 252501 (2012).
 - [10] J. A. Tostevin and A. Gade, *Phys. Rev. C* **103**, 054610 (2021).
 - [11] J. A. Tostevin and A. Gade, *Phys. Rev. C* **90**, 057602 (2014).

- [12] T. Aumann *et al.*, *Prog. Part. Nucl. Phys.* **118**, 103847 (2021).
- [13] CLAS Collaboration, *Nature (London)* **560**, 617 (2018).
- [14] Ø. Jensen, G. Hagen, M. Hjorth-Jensen, B. A. Brown, and A. Gade, *Phys. Rev. Lett.* **107**, 032501 (2011).
- [15] J. Lee *et al.*, *Phys. Rev. Lett.* **104**, 112701 (2010).
- [16] J. Lee *et al.*, *Phys. Rev. C* **83**, 014606 (2011).
- [17] L. Atar *et al.*, *Phys. Rev. Lett.* **120**, 052501 (2018).
- [18] M. Holl *et al.*, *Phys. Lett. B* **795**, 682 (2019).
- [19] M. Gómez-Ramos and A. M. Moro, *Phys. Lett. B* **785**, 511 (2018).
- [20] A. Leistenschneider *et al.*, *Phys. Rev. C* **65**, 064607 (2002).
- [21] J. M. Boillos *et al.*, *Phys. Rev. C* **105**, 014611 (2022).
- [22] A. Gade *et al.*, *Phys. Rev. C* **77**, 044306 (2008).
- [23] E. C. Simpson and J. A. Tostevin, *Phys. Rev. C* **79**, 024616 (2009).
- [24] Y. X. Zhao *et al.*, *Phys. Rev. C* **100**, 044609 (2019).
- [25] Y. Z. Sun *et al.*, *Phys. Rev. C* **104**, 014310 (2021).
- [26] E. K. Warburton and B. A. Brown, *Phys. Rev. C* **46**, 923 (1992).
- [27] N. Shimizu *et al.*, *Comput. Phys. Commun.* **244**, 372 (2019).
- [28] NuDat 3.0, <https://www.nndc.bnl.gov/nudat3/>, accessed 18 May, 2022
- [29] C. A. Bertulani and A. Gade, *Comput. Phys. Commun.* **175**, 372 (2006).
- [30] J. A. Tostevin, *Nucl. Phys. A* **682**, 320 (2001).
- [31] B. A. Brown, *Phys. Rev. C* **58**, 220 (1998).
- [32] L. Ray, *Phys. Rev. C* **20**, 1857 (1979).
- [33] S. K. Charagi and S. K. Gupta, *Phys. Rev. C* **41**, 1610 (1990).
- [34] S. M. Lenzi, A. Vitturi, and F. Zardi, *Phys. Rev. C* **40**, 2114 (1989).
- [35] W. Horiuchi, Y. Suzuki, B. Abu-Ibrahim, and A. Kohama, *Phys. Rev. C* **75**, 044607 (2007).
- [36] W. H. Press *et al.*, *Numerical Recipes in C: The Art of Scientific Computing*, 2nd ed. (Cambridge University Press, Cambridge, 1992), p. 383.
- [37] Z. Y. Sun *et al.*, *Phys. Rev. C* **90**, 037601 (2014).
- [38] J. L. Li, C. A. Bertulani, and F. R. Xu, *Phys. Rev. C* **105**, 024613 (2022).
- [39] C. A. Bertulani, A. Idini, and C. Barbieri, *Phys. Rev. C* **104**, L061602 (2021).
- [40] Y. P. Xu *et al.*, *Chin. Phys. C* **46**, 064102 (2022).
- [41] V. Panin *et al.*, *Phys. Lett. B* **753**, 204 (2016).
- [42] C. Louchart, A. Obertelli, A. Boudard, and F. Flavigny, *Phys. Rev. C* **83**, 011601(R) (2011).